Free Radical Biology and Medicine 70 (2014) 14–22

Contents lists available at ScienceDirect

Free Radical Biology and Medicine

journal homepage: www.elsevier.com/locate/freeradbiomed

Original Contribution

Proopiomelanocortin gene delivery induces apoptosis in melanoma through NADPH oxidase 4-mediated ROS generation

Guei-Sheung Liu [a,b,1], Jian-Ching Wu [c,1], Han-En Tsai [d], Gregory J. Dusting [a,b], Elsa C. Chan [a,b], Chieh-Shan Wu [e,**], Ming-Hong Tai [c,d,f,*]

[a] Centre for Eye Research Australia, Melbourne, VIC 3002, Australia
[b] Department of Ophthalmology, University of Melbourne, Melbourne, VIC 3002, Australia
[c] Doctoral Degree Program in Marine Biotechnology, National Sun Yat-sen University and Academia Sinica, Kaohsiung 804, Taiwan
[d] Institute of Biomedical Science, and National Sun Yat-sen University, Kaohsiung 804, Taiwan
[e] Department of Dermatology, Kaohsiung Veterans General Hospital, Kaohsiung 813, Taiwan
[f] Center for Neuroscience, National Sun Yat-sen University, Kaohsiung 804, Taiwan

ARTICLE INFO

Article history:
Received 26 August 2013
Received in revised form
3 December 2013
Accepted 21 December 2013
Available online 8 January 2014

Keywords:
POMC
Melanoma
Apoptosis
ROS
NADPH oxidase
Free radicals

ABSTRACT

Hypoxia in the tumor microenvironment triggers differential signaling pathways for tumor survival. In this study, we characterize the involvement of hypoxia and reactive oxygen species (ROS) generation in the antineoplastic mechanism of proopiomelanocortin (POMC) gene delivery in a mouse B16-F10 melanoma model in vivo and in vitro. Histological analysis revealed increased TUNEL-positive cells and enhanced hypoxic activities in melanoma treated with adenovirus encoding POMC (Ad-POMC) but not control vector. Because the apoptotic cells were detected mainly in regions distant from blood vessels, it was hypothesized that POMC therapy might render melanoma cells vulnerable to hypoxic insult. Using a hypoxic chamber or cobalt chloride ($CoCl_2$), we showed that POMC gene delivery elicited apoptosis and caspase-3 activation in cultured B16-F10 cells only under hypoxic conditions. The apoptosis induced by POMC gene delivery was associated with elevated ROS generation in vitro and in vivo. Blocking ROS generation using the antioxidant *N*-acetyl-L-cysteine abolished the apoptosis and caspase-3 activities induced by POMC gene delivery and hypoxia. We further showed that POMC-derived melanocortins, including α-MSH, β-MSH, and ACTH, but not γ-MSH, contributed to POMC-induced apoptosis and ROS generation during hypoxia. To elucidate the source of ROS generation, application of the NADPH oxidase inhibitor diphenyleneiodonium attenuated α-MSH-induced apoptosis and ROS generation, implicating the proapoptotic role of NADPH oxidase in POMC action. Of the NADPH oxidase isoforms, only Nox4 was expressed in B16-F10 cells, and Nox4 was also elevated in Ad-POMC-treated melanoma tissues. Silencing Nox4 gene expression with Nox4 siRNA suppressed the stimulatory effect of α-MSH-induced ROS generation and cell apoptosis during hypoxia. In summary, we demonstrate that POMC gene delivery suppressed melanoma growth by inducing apoptosis, which was at least partly dependent on Nox4 upregulation.

Hypoxia plays a critical role in cancer development and progression. Low oxygen concentrations in the tumor microenvironment facilitate recruitment of vascular endothelial cells and promote angiogenesis to supply oxygen and nutrients to tumor cells. To adapt metabolically to hypoxic conditions, tumor cells also exhibit increased glucose transport and anaerobic glycolysis [1]. Fifty to sixty percent of locally advanced solid tumors, including melanomas, are characterized by areas of hypoxia/anoxia that result from an imbalance between oxygen supply and consumption in proliferating tumor cells. This imbalance is further exacerbated by a compromised tumor vasculature [2]. Studies have shown that the presence of hypoxia within a tumor is an independent marker of a poor prognosis for patients with various cancer types including cutaneous melanomas [3]. Because stringent hypoxia/anoxia ($< 0.5\%$ O_2) is toxic for normal and tumor cells, it can promote tumor progression by selecting cells with mutations that allow them to survive under these extreme conditions [4]. Furthermore, hypoxia activates signaling pathways that trigger neovascularization and facilitates tumor cell invasion, migration, adhesion, and metastasis [5].

* Corresponding author. National Sun Yat-sen University, Institute of Biomedical Science, 70 Lien-Hai Road, Kaohsiung 804, Taiwan. Fax: +886 7 5250197
** Corresponding author. Fax: +886 7 3468209
[1] These authors contributed equally to this work.

http://dx.doi.org/10.1016/j.freeradbiomed.2013.12.024
0891-5849

Reactive oxygen species (ROS) are oxygen-containing, short-lived molecules that are highly reactive. The most common examples include superoxide, hydrogen peroxide (H_2O_2), hydroxyl radical ($^{\bullet}OH$), nitric oxide (NO), and peroxynitrite ($ONOO^-$). ROS are generally considered unwanted by-products produced from aerobic metabolism; for instance, superoxide is produced during mitochondrial oxidative phosphorylation [6]. Various enzyme systems produce ROS, including the mitochondrial electron transport chain, cytochrome P450, lipooxygenase, cyclooxygenase, NADPH oxidase complex, xanthine oxidase, and peroxisomes [7]. ROS are increased in malignant cells in part as a result of oncogene signaling via the NADPH oxidase complex and by hypoxia-related mitochondrial ROS. Increased oxidant levels contribute to enhanced cell proliferation and suppression of apoptosis. Oxygen depletion stimulates mitochondria to produce ROS [8], which activate signaling pathways involving hypoxia-inducible factor 1α, which in turn promote cancer cell survival and tumor growth [9,10]. However, an overproduction of ROS can cause apoptosis by opening the mitochondrial permeability transition pore and thus releasing proapoptotic factors [11,12]. How cancer cells manage the balance of ROS during cancer development still remains unclear.

Proopiomelanocortin (POMC) is a stress hormone and is processed into various neuropeptides including adrenocorticotrophic hormone (ACTH); α-, β-, and γ-melanocyte-stimulating hormone (MSH); and β-endorphin through POMC-processing enzymes such as prohormone convertases 1 and 2. POMC-derived peptides possess pleiotropic functions, including pigmentation, adrenocortical function, regulation of energy homeostasis, and immunity modulation, in the central and peripheral systems [13–16]. A POMC-derived peptide, α-MSH, has been reported to trigger melanoma and melanocyte differentiation [17] and potently inhibits migration and invasion of B16-BL6 melanoma cells in vitro and in vivo [18]. These findings suggest that POMC expression may inhibit the tumorigenicity of tumors.

We and others recently showed that targeted gene therapy with POMC suppressed the growth of melanoma and lung cancer in animals [19–21]. In this study, we therefore characterized the tumor-suppressive mechanisms of POMC in a mouse model of melanoma in vivo and in vitro, by overexpressing POMC using adenoviruses carrying the POMC gene. We first characterized the effects of POMC overexpression on cell apoptosis and then explored how POMC overexpression caused apoptosis under hypoxia. We identified a novel tumor-suppressive mechanism of POMC that facilitates cell apoptosis through modulation of the ROS-inducing enzyme NADPH oxidase 4 (Nox4) in melanoma. POMC gene delivery may represent a novel therapeutic avenue for the treatment of melanoma.

Materials and methods

Preparation of adenovirus vectors

To overexpress POMC in B16-F10 melanoma cells, cells were infected with recombinant adenoviruses containing the POMC gene (Ad-POMC) or control green fluorescent protein (Ad-GFP). Ad-GFP and Ad-POMC were generated as previously described [22].

Primary melanoma models and gene delivery

All animal experiments were carried out under protocols approved by the Institutional Animal Care and Use Committee of National Sun Yet-Sen University. To induce the primary melanoma, B16-F10 cells were subcutaneously injected into C57BL/6 mice (5×10^5 cells in 0.1 ml of phosphate-buffered saline (PBS); $n = 13–15$) to monitor tumor growth. After tumors had grown to at least 100 mm^3 (10 days after implantation), the mice were administered adenoviral vector at the indicated doses in 0.1 ml of PBS via intratumoral injection. Subsequently, tumor volumes were measured with a dial-caliper according to the following formula: $width^2 \times length \times 0.52$. For tumor-suppressing studies, experiments were terminated when the tumor burden exceeded 10% of the animal's normal body weight.

Terminal deoxynucleotidyl transferase (TdT)-mediated dUTP nick-end labeling (TUNEL) assay

B16-F10 melanoma cells were implanted at day 0 and treated with intravenous injection of adenovirus vectors at day 10. After treatment for 21 days, cell death in frozen mouse melanoma sections was detected by enzyme labeling of DNA strand breaks using a TUNEL assay (*In Situ* Cell Death Detection Kit; Roche, Basel, Switzerland) according to the manufacturer's instructions. Briefly, sections were incubated with a mixture of TdT and fluorescein–dUTP to react at 37 °C to label free 3′-OH ends of genomic DNA. After TUNEL staining, the sections were counterstained with propidium iodide (PI; 500 ng/ml) for 30 min at 25 °C and viewed under a fluorescence microscope. For quantifying the immunostaining of TUNEL, each sample was randomly captured by microscopy for at least five independent fields. An apoptotic index was estimated by normalizing the number of TUNEL-positive cells to the total number of PI-positive cells and calculated from five independent fields with a 40× microscopic field.

In situ detection of hypoxia

Cells undergoing hypoxia and apoptosis in mouse tumor tissue sections were detected using pimonidazole (Hypoxyprobe-1; Hypoxyprobe, Burlington, MA, USA) and a TUNEL kit according to the manufacturer's instructions. Sections were then counterstained with DAPI.

Cell cultures and reagents

Mouse (B16-F10) and human (A375 and A2058) melanoma cells, mouse fibroblast cells (NIH3T3), and rat hepatocytes (clone 9) were purchased from the American Type Culture Collection (Manassas, VA, USA) and cultured and maintained in complete medium made up of Dulbecco's modified Eagle's medium (Invitrogen, Carlsbad, CA, USA) with 10% fetal bovine serum (FBS; Hyclone, Logan, UT, USA), 2 mM glutamine, 100 mg/ml streptomycin (Invitrogen), and 100 U/ml penicillin, at 37 °C in a 5% CO_2 atmosphere. ACTH, α-MSH, β-MSH, and γ-MSH were purchased from Bachem (Torrance, CA, USA). Cobalt chloride ($CoCl_2$), diphenyleneiodonium chloride (DPI), rotenone, allopurinol, 2′,7′-dichlorodihydrofluorescein diacetate (DCFH-DA), dihydroethidium (DHE), *N*-acetyl-L-cysteine (NAC), and indomethacin were purchased from Sigma–Aldrich (St. Louis, MO, USA).

Treatment of hypoxia

To mimic hypoxic conditions, cells were incubated in a commercially available hypoxia system (< 1% oxygen), GENbox Jar (BioMerieux), used as previously described [23], or treated with a pharmacological agent, $CoCl_2$ (100 μM), at 37 °C. The duration of hypoxia treatment was between 48 and 72 h depending on experimental conditions as described below.

Cell cycle analysis

B16-F10 cells were infected with Ad-POMC and Ad-GFP at a multiplicity of infection (m.o.i.) of 1000 for 48 h. After infection, the cells were maintained in complete medium with reduced FBS (1%) for hypoxia treatments. Cells were harvested, washed twice with PBS before fixation with ice-cold ethanol (70%), and then stored overnight at −20 °C. Cells were washed twice with PBS before incubation with RNase A (10 μg/ml) and PI (50 μg/ml) for 30 min at 37 °C. The DNA content of 20,000 events was analyzed using a FACSCalibur flow cytometer (Becton Dickinson Biosciences; San Jose, CA, USA) and CELLQuest software.

Measurement of ROS generation by 2′,7′-dichlorofluorescein diacetate (DCF-DA)

Intracellular ROS concentration was measured using DCF-DA as previously described [24]. For gene delivery, cells (1×10^5 cells/well) were seeded in six-well plates and subjected to infection with adenovirus vectors at an m.o.i. of 1000 for 24 h and hypoxia treatment for another 24 h before DCF-DA. For peptide treatment, B16-F10 cells (1×10^5 cells/well) were seeded in six-well plates and pretreated with ACTH, α-MSH, β-MSH, and γ-MSH (10 nM) for 24 h and then incubated with $CoCl_2$ (100 μM) for another 24 h before DCF-DA. Cells were rinsed with HBSS (Hanks' balanced salt solution), loaded with DCF-DA (10 μM), and incubated for 15 min at 37 °C. DCF fluorescent signals were detected immediately by FACSCalibur flow cytometer (Becton Dickinson Biosciences) and CELLQuest software.

Hydrogen peroxide measurement by Amplex red

Extracellular H_2O_2 was detected using Amplex red assay as previously described [24]. For gene delivery, cells (1×10^5 cells/well) were seeded in six-well plates and subjected to infection with adenovirus vectors at an m.o.i. of 1000 for 24 h and hypoxia treatment for another 24 h before Amplex red assay. For peptide treatment, cells (1×10^5 cells/well) were seeded in six-well plates and pretreated with ACTH, α-MSH, β-MSH, and γ-MSH (10 nM) for 24 h and then incubated with $CoCl_2$ (100 μM) for another 24 h before Amplex red assay. After treatment, cells were suspended in Krebs–Hepes buffer (HBSS, 98 mM NaCl, 4.7 mM KCl, 25 mM $NaHCO_3$, 1.2 mM $MgSO_4$, 1.2 mM KH_2PO_4, 2.5 mM $CaCl_2$, 11.1 mM D-glucose, and 20 mM Hepes–Na) containing Amplex red reagent (Invitrogen). Fluorescence was then measured with excitation and emission at 480 and 530 nm, respectively, using a Polarstar microplate reader (BMG Labtech) at 37 °C.

In situ superoxide detection

The superoxide in frozen tumor sections was detected by DHE (5 μM) as previously described [25]. Briefly, after TUNEL staining, the sections were incubated with DHE for 30 min at 37 °C in a humidified chamber protected from light. The red fluorescence was detected using a fluorescence microscope (DP70; Olympus, Tokyo, Japan).

Caspase-3 activity assay

Caspase-3 activity was measured using the CaspACE Assay System, colorimetric kit (Promega, Madison, WI, USA). Briefly, cells (2×10^5 cells/well) were seeded in a six-well tissue culture plate (Falcon, Franklin Lakes, NJ, USA). After an infection with adenovirus vectors at an m.o.i. of 1000 for 24 h, cells were incubated with $CoCl_2$ (100 μM) and in the absence or presence of NAC (10 mM) in 1% FBS medium for 24 h. The lysate (100 μg) was added to the CaspACE assay buffer containing the caspase-3 substrate Ac-DEVD-*p*-nitroaniline and incubated for 4 h at 37 °C. Cells treated with dimethyl sulfoxide were used as controls. Absorbance at 405 nm was read by a scanning multiwell spectrophotometer (Dynatech Laboratories, Chantilly, VA, USA).

Western blot

Cell lysates were prepared and protein expression was measured as previously described [22]. The PVD membrane was blocked with 5% milk in Tris-buffered saline–Tween 20 for 1 h and then incubated with specific primary antibodies against Nox4 (1:500 dilution; Santa Cruz Biotechnology, Santa Cruz, CA, USA) and β-actin antibodies (1:10,000 dilution; Sigma) for 1 h at room temperature. After incubation with secondary antibody conjugated with horseradish peroxidase (HRP; 1:10,000 dilution in 5% milk) for 1 h, signals on the membrane were detected using chemiluminescent HRP substrate (Millipore Corp.; Billerica, MA, USA) and exposed to X-ray film for autoradiograms.

Quantitative real-time PCR

RNA was isolated from B16-F10 cells using RNAzol according to the manufacturer's instructions (Tel-Test, Friendswood, TX, USA). Two micrograms of total RNA was used for reverse transcription with SuperScript III (Invitrogen) using olio(dT) and random primers. For quantitative real-time PCR, reactions were performed in an ABI Prism 7700 system (Applied Biosystems, Foster City, CA, USA) using the SYBR Green PCR master mix and the predesigned gene-specific probe and primer sets for mouse Nox4 (NM_015760.4). Data were normalized to β-actin (NM_007393.3) and expressed as fold changes over that in the control experiments. The primer sequences were as follows: Nox4 forward primer, 5′-CTCAACTGCAGCCTCATCCTT-3′, and reverse primer, 5′-ACTGAAAAGTTGAGGGCATTCAC-3′; β-actin forward primer, 5′-GGAATCCTGTGGCATCCAT-3′, and reverse primer, 5′-GCTCAGGAGGAGCAATGAT-3′.

RNA interference

To knock down the gene expression of Nox4 we purchased small interfering RNA (siRNA) from Santa Cruz Biotechnology. Cells were transfected for 4 h and then incubated with complete medium for 48 h. After transfection, the cells were pretreated with $CoCl_2$ for 1 h before treatment with and without α-MSH (10 nM) for 24 h before cell harvest.

Statistical analysis

Data are presented as the mean ± standard error of the mean (SEM). The mean data were analyzed with one-way analysis of variance followed by Newman–Keuls post hoc or *t* test (for multiple comparisons). A p value of less than 0.05 was regarded as statistically significant.

Results

POMC gene delivery induces apoptosis in melanoma

To evaluate the therapeutic potential of POMC gene delivery, mice bearing established melanoma were administered adenoviral vector and then monitored for tumor progression. Mice treated with Ad-POMC showed significantly retarded melanoma growth compared with control animals (Supplementary Fig. 1). To investigate the mechanism of POMC gene delivery on inhibition of tumor growth, tumor tissues were collected and subjected to

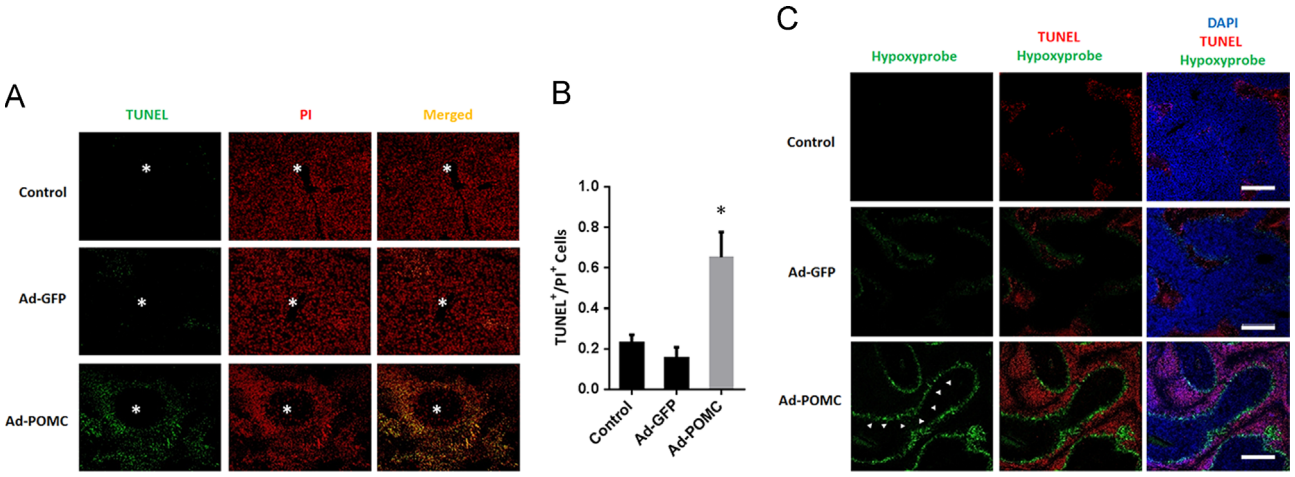

Fig. 1. Effect of systemic POMC overexpression on apoptosis in melanoma tissue. (A) The representative profiles of TUNEL staining in Ad-GFP- and Ad-POMC-treated melanoma. Apoptotic cells in melanoma were detected by TUNEL staining (green) and the cell nucleus was counterstained with propidium iodide (PI; red). (B) Quantification of apoptotic index in Ad-POMC- and Ad-GFP-treated melanoma. The apoptotic index is expressed as the ratio of the number of TUNEL-positive cells to the number of PI-positive cells. Data are expressed as mean ± SEM from 6 experiments. (C) Correlation of apoptosis and hypoxia in melanoma. Hypoxia activity and apoptosis in melanoma tissues were detected by the Hypoxyprobe-1 kit (pimonidazole; green) and TUNEL (red) assay, respectively, followed by counterstaining with DAPI (blue). Arrows indicate hypoxic cells. Scale bar, 20 μm. $*p < 0.05$.

histological analysis. Fluorescence images in Fig. 1A demonstrate an accumulation of TUNEL-positive cells in tumor nodules surrounding blood vessels in Ad-POMC-infected tumors, whereas few apoptotic cells were found in Ad-GFP-infected melanoma. Quantification analysis of apoptotic events confirmed that the apoptotic index in Ad-POMC-infected melanoma was significantly higher than that in Ad-GFP-infected tumors (Fig. 1B).

POMC gene delivery induces apoptosis in melanoma cells under a hypoxic challenge

Because TUNEL-positive apoptotic cells were detected predominantly in the ischemic region distant from blood vessels, POMC gene therapy seems to render melanoma cells susceptible to hypoxic challenge. To address this aim, the extent of hypoxia in tumor sections was detected with immunofluorescence microscopy using a conventional Hypoxyprobe-1 kit. Ad-POMC-infected tumor sections demonstrated a greater degree of hypoxia in comparison to Ad-GFP-infected tissues (Fig. 1C). To examine whether cells undergoing apoptosis correlate with tissue hypoxia, tumor sections were costained with TUNEL and Hypoxyprobe-1 probe. It was found that ischemic activity was localized in close proximity to TUNEL-positive cells in Ad-POMC-infected tumors. Although there was little hypoxic or TUNEL-positive signal in Ad-GFP tumors, the distribution patterns of both signals were similar to those of Ad-POMC-infected tumors, suggesting that induction of apoptosis tends to occur in hypoxic regions.

Having established that the induction of cell apoptosis by systemic POMC gene delivery was associated with tissue hypoxia, we explored the mechanism underlying such process in B16-F10 melanoma cells. We used a hypoxia chamber (< 1% oxygen) and a pharmacological agent, $CoCl_2$ (100 μM), to mimic hypoxic conditions. Flow cytometry analysis demonstrated that the proportion of apoptotic cells was increased about 12% in the Ad-POMC-infected group in a hypoxia chamber (Fig. 2A). Cells treated with $CoCl_2$ analyzed by flow cytometry analysis also showed an increase in apoptotic cells in the Ad-POMC group compared to the Ad-GFP group (Fig. 2B). The stimulatory effect of POMC gene delivery on apoptosis in B16-F10 cells was further confirmed by evaluating the caspase-3 activity. As shown in Fig. 2C, Ad-POMC induced an increase in caspase-3 activity in $CoCl_2$-induced hypoxia. Taken together, these results suggested that POMC gene delivery triggers melanoma cells toward programmed cell death under hypoxic challenges.

Melanocortins promote apoptosis of melanoma cells under hypoxia

Our previous study demonstrated that POMC-derived peptides (α-MSH, β-MSH, and ACTH) reduced colony formation and invasive potential in B16-F10 melanoma cells [19]. In this study, we characterize which POMC-derived peptides induced apoptosis in B16-F10 melanoma cells. To address this aim, cells were treated with 10 nM α-MSH, β-MSH, ACTH, and γ-MSH under $CoCl_2$-induced hypoxic conditions. In flow cytometry analysis, α-MSH, β-MSH, and ACTH peptides enhanced the G0/G1-phase population through a reduction in cell numbers in S and M phases in normoxia, indicating cell cycle arrest (Supplementary Table 1). However, under hypoxia conditions, α-MSH, β-MSH, and ACTH peptides remarkably induced about 12% of the population of apoptotic cells in pre-G0 phase, whereas γ-MSH had no such effect (Fig. 3). A similar effect was observed in two human melanoma cell lines (A375 and A2058), but not in two nontransformed cell lines (NIH3T3 and clone 9) (Supplementary Fig. 2). Therefore, we identified that α-MSH, β-MSH, and ACTH but not γ-MSH induced apoptosis in melanoma cells during hypoxia, which shows selectivity on melanoma cells.

Excessive ROS generation participated in POMC-induced apoptosis during hypoxia

Having established that POMC overexpression potentiated the effect of hypoxia on apoptosis of melanoma cells, we investigated the molecular mechanisms underlying such process. ROS have been implicated in the regulation of apoptosis in melanoma cells [26,27]. We therefore performed in situ detection of superoxide with DHE and TUNEL assay to assess the distribution of ROS production and cell apoptosis in Ad-POMC- and Ad-GFP-treated melanoma tissues. There was an accumulation of DHE fluorescence distant from the blood vessel to the far tumor region and such signal was colocalized with TUNEL-positive staining cells in the Ad-POMC-treated group (Fig. 4A). Little DHE fluorescence was detected in Ad-GFP-treated melanoma tissues, suggesting that ROS generation is associated with cell apoptosis in melanoma (Fig. 4A). To elucidate a role for ROS generation in POMC-mediated cell

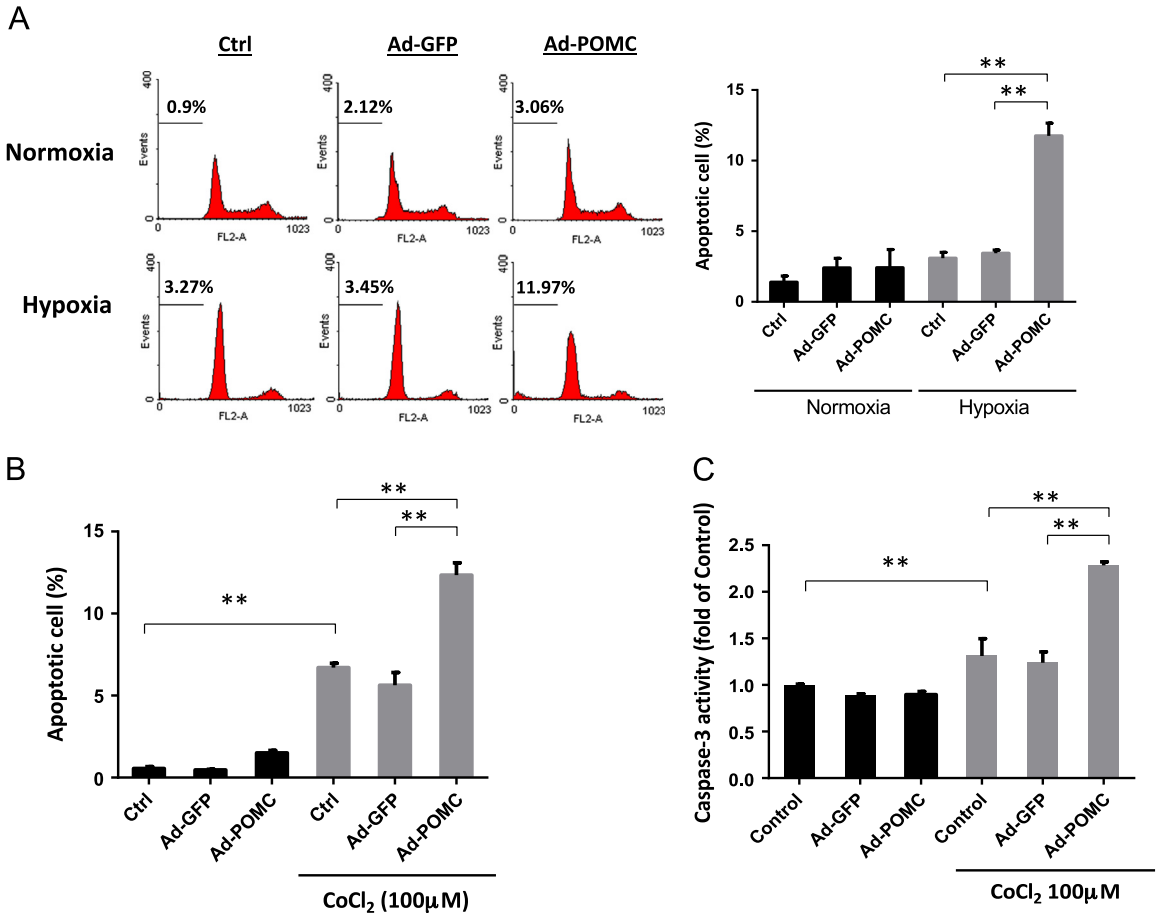

Fig. 2. Effect of POMC expression on sensitivity of melanoma cells to hypoxia. (A) Flow cytometry analysis of cells obtained from pre-G0 phase shows that Ad-POMC gene delivery increased apoptotic cells compared to the Ad-GFP group in the hypoxia chamber. (B) Effect of hypoxia mimetic $CoCl_2$ on cell apoptosis. (C) POMC gene delivery triggered caspase-3 cascade activation in B16-F10 melanoma cells during hypoxia. The ratio of caspase-3 activity was measured by colorimetric caspase-3 activation assay. Data are expressed as means ± SEM from triplicate experiments. $^{**}p < 0.01$.

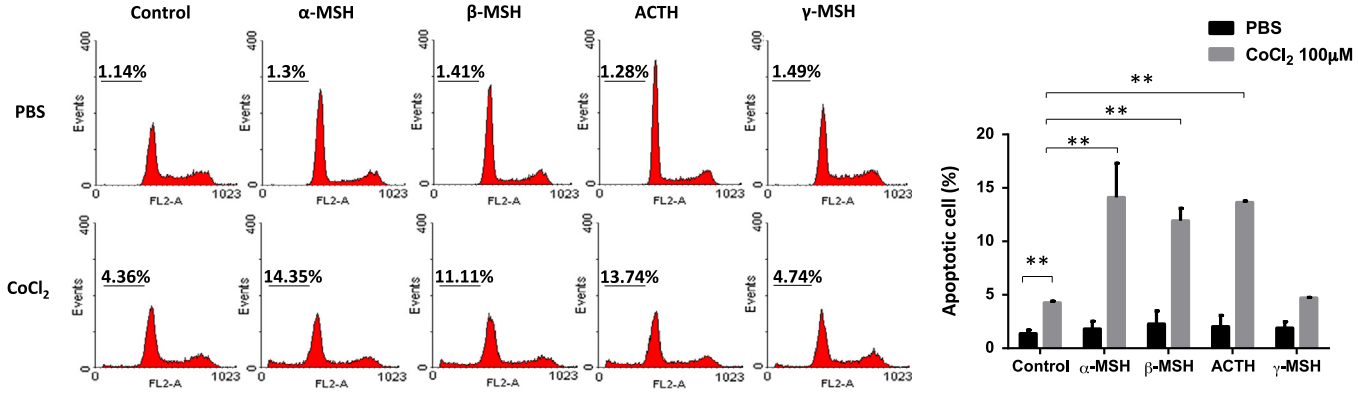

Fig. 3. The effect of POMC-derived peptides on sensitivity of melanoma cells to hypoxia. Representative flow cytometry demonstrating the effects of α-MSH, β-MSH, ACTH, and γ-MSH neuropeptides (10 nM for each peptide) on cell populations under normal and $CoCl_2$-induced hypoxic conditions. The percentage of apoptotic cells is expressed as means ± SEM from triplicate experiments. $^{**}p < 0.01$.

apoptosis under hypoxia, we first examined the effect of POMC overexpression on ROS generation in B16-F10 melanoma cells under normal and $CoCl_2$-induced hypoxic conditions. Hypoxia increased total ROS production detected by DCF-DA in control and Ad-GFP infected cells, which was potentiated by an overexpression of POMC in melanoma cells infected with Ad-POMC (Fig. 4B). There was a tendency of increased H_2O_2 generation in hypoxic cells and such increase was potentiated by Ad-POMC treatment (Fig. 4C). Moreover, inhibition of ROS production with an antioxidant, NAC (10 mM), was found to abrogate the Ad-POMC-stimulated augmentation of caspase-3 activity and also rescued the Ad-POMC-induced apoptosis comparison with the Ad-GFP group during hypoxia (Figs. 4D and 4E), indicating that ROS production contributed to Ad-POMC-induced apoptosis. In summary, our results suggested that ROS production by POMC gene delivery was involved in apoptosis in melanoma cells during hypoxia.

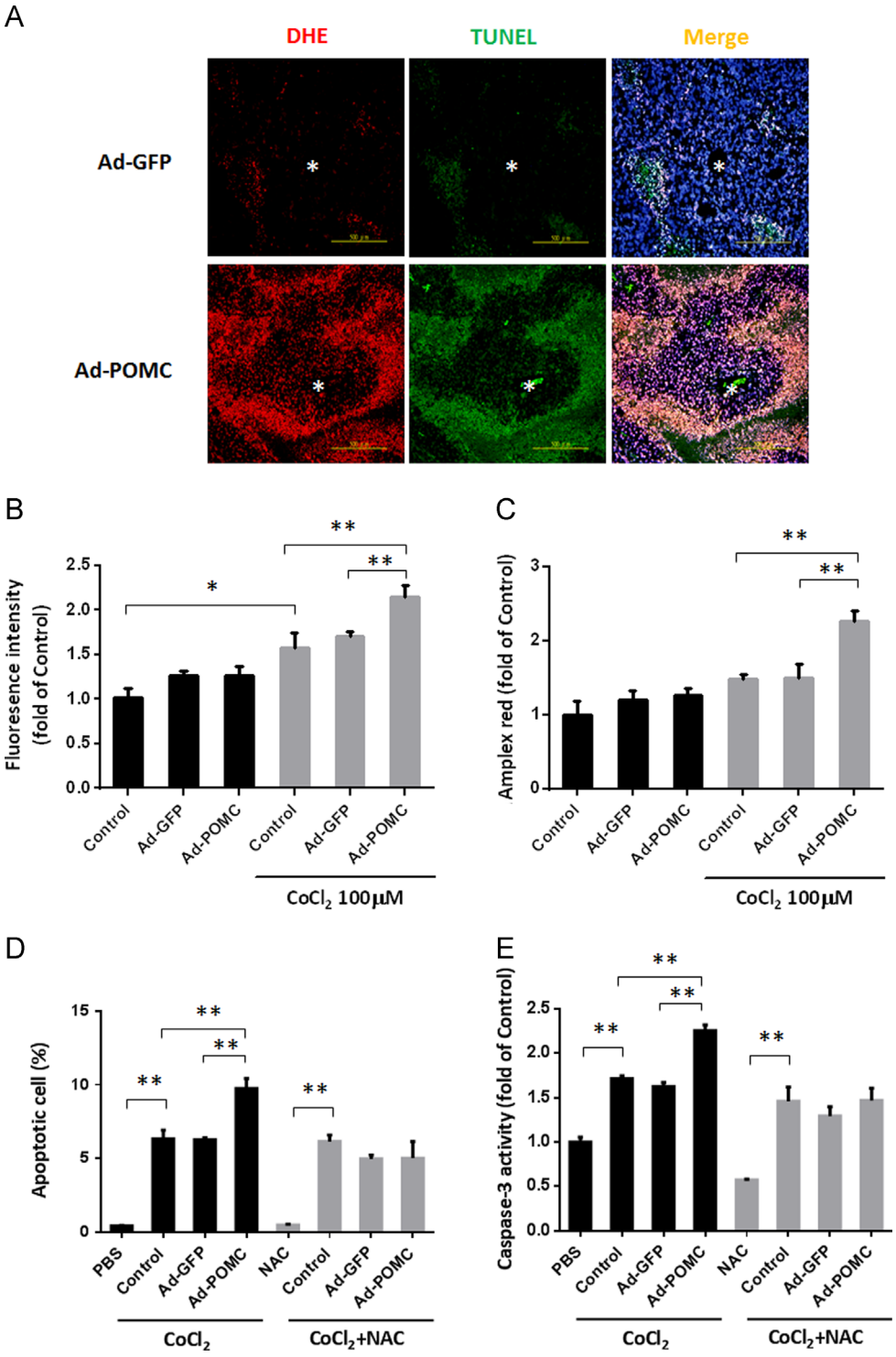

Fig. 4. Excess ROS production by POMC gene delivery triggered the apoptotic process in B16-F10 melanoma cells during hypoxia. (A) Representative profiles of TUNEL and DHE costaining in Ad-GFP- and Ad-POMC-treated melanoma. The apoptotic cells in melanoma were detected by TUNEL staining (green) and the cellular superoxide anion (O_2^-) is indicated with DHE (red). The cell nucleic acids were counterstained with DAPI (blue). Scale bar, 500 μm. (B) Measurement of intracellular ROS generation by DCF-DA staining. (C) The extracellular H_2O_2 production was measured by Amplex red assay. (D) Flow cytometry analysis shows that blocking ROS generation with NAC (10 mM) could rescue Ad-POMC-induced apoptosis in hypoxia. (E) The ratio of caspase-3 activity was measured by colorimetric caspase-3 activation assay. Data are expressed as means ± SEM from triplicate experiments. $^*p < 0.05$, $^{**}p < 0.01$. (For interpretation of the references to color in this figure legend, the reader is referred to the web version of this article.)

Melanocortins increased ROS generation in melanoma cells during hypoxia

We next examined which of the POMC-derived peptides elevated ROS generation in melanoma cells during hypoxia. To address this question, cells were treated with one of the POMC-derived peptides, α-, β-, and γ-MSH and ACTH (10 nM) for 24 h and then incubated with $CoCl_2$ (100 μM) for another 24 h before assessment of ROS production with DCF-DA and Amplex red assays. As shown in Fig. 5A, $CoCl_2$-induced hypoxia stimulated DCF-DA signals in melanoma cells and such induction was significantly potentiated by α-MSH, β-MSH, and ACTH but not γ-MSH. H_2O_2 generation was also

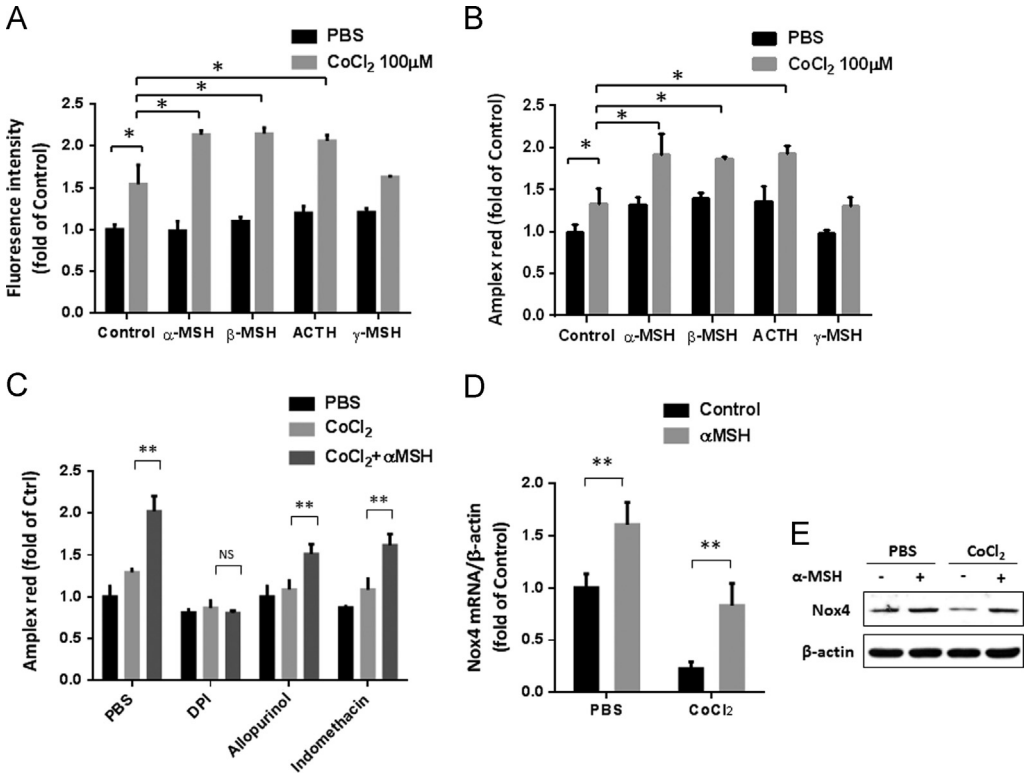

Fig. 5. Effect of POMC-derived peptides on ROS generation and association with an upregulation of Nox4 in hypoxia. (A, B) Clarification of POMC-derived peptide α-MSH, β-MSH, ACTH, and γ-MSH (10 nM) capability to stimulate ROS generation by DCFH-DA and Amplex red assay. (C) The source of ROS generation. Analysis of ROS generation in the absence and presence of DPI (0.1 μM), allopurinol (50 μM), and indomethacin (1 μM) after α-MSH stimulation by Amplex red assay. (D and E) The effect of α-MSH on Nox4 gene and protein expression in the absence or presence $CoCl_2$ (100 μM). Data are expressed as means ± SEM from triplicate experiments. $^{*}p < 0.05$, $^{**}p < 0.01$.

augmented by α-MSH, β-MSH, and ACTH peptides in the $CoCl_2$ group (Fig. 5B). Our results suggested that POMC-derived peptides (α-MSH, β-MSH, and ACTH) contributed to ROS generation in melanoma during hypoxia.

ROS generation is mediated though α-MSH-induced Nox4 NADPH oxidase upregulation

α-MSH was found to modulate the inhibitory effect of systemic POMC delivery on the progression of melanoma [19]. We therefore used α-MSH peptide to investigate the source of ROS generation in cell apoptosis during hypoxia. Several endogenous enzymes, including xanthine oxidase [28], mitochondrial enzymes [29], cyclooxygenase [30], and NADPH oxidase [31], have been implicated as sources of ROS generation in melanoma cells. To investigate which enzyme sources were involved in α-MSH-mediated ROS generation during hypoxia, cells were treated with a pharmacological inhibitor of these enzymes 10 min before Amplex red assay (Fig. 5C). None of the inhibitors affected basal H_2O_2 generation. The inhibitor of NADPH oxidase, DPI (0.1 μM), significantly abrogated α-MSH-induced ROS generation during hypoxia. In contrast, inhibitors of xanthine oxidase (allopurinol, 50 μM) and cyclooxygenase (indomethacin, 1 μM) did not affect the stimulatory effect of α-MSH on H_2O_2 production, suggesting NADPH oxidase was a major source of α-MSH-mediated ROS generation in melanoma cells. We further investigated which of the NADPH oxidase isoforms was involved in α-MSH-induced ROS production. By using quantitative PCR and Western blot analysis of NADPH oxidase isoforms (Nox1 to Nox4), we first characterized the Nox4 expression in B16-F10 melanoma cells (Supplementary Fig. 3). Moreover, α-MSH enhanced Nox4 at the mRNA and protein levels, whereas other NADPH oxidase isoforms (Nox1, Nox2, and Nox3) remained undetected. Interestingly, α-MSH reversed the inhibitory effect of hypoxia on Nox4 expression (Figs. 5D and E), suggesting that the stimulatory effect of α-MSH on ROS generation under hypoxic conditions was associated with an upregulation of Nox4 expression.

Silencing Nox4 gene expression rescues α-MSH-induced apoptosis during hypoxia

To investigate the role of Nox4 in α-MSH-induced apoptosis during hypoxia, gene silencing of Nox4 with siRNA was performed in B16-F10 melanoma cells. We first verified that transfection of Nox4 siRNA but not control siRNA significantly attenuated the mRNA and protein expression of Nox4 (Fig. 6A). Nox4 siRNA also remarkably abolished the intracellular and extracellular H_2O_2 generation and inhibited the stimulatory effect of hypoxia on ROS generation (Fig. 6B). Importantly, silencing of Nox4 gene expression successfully alleviated α-MSH-induced apoptosis during hypoxia (Fig. 6C). Moreover, immunostaining analysis revealed that Nox4 staining has strong fluorescence intensity in the Ad-POMC-infected group and displayed a positive correlation with TUNEL staining compared to the Ad-GFP-infected group (data not shown). In summary, these results indicated that ROS derived from Nox4 are involved in α-MSH-induced apoptosis in melanoma cells during hypoxia.

Discussion

In this study we clarified how Nox4-mediated ROS generation was a key signaling pathway involved in cell apoptosis mediated by POMC gene delivery in melanoma during hypoxic insults. Our results provide further understanding of the tumor-suppressive mechanisms of POMC for treatment of melanoma.

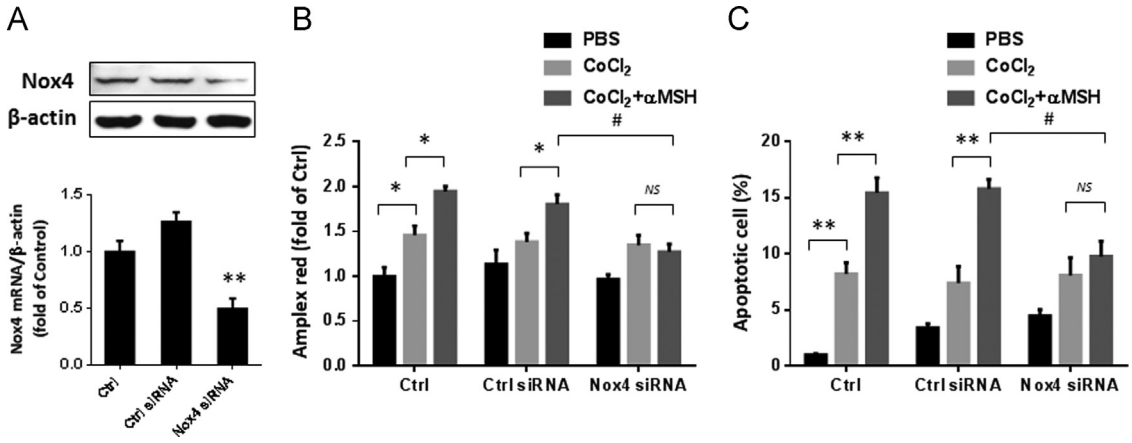

Fig. 6. Effect of Nox4 silencing on ROS generation and apoptosis in B16-F10 melanoma cells. Cells were transfected with control siRNA or Nox4 siRNA for 48 h before cell harvest. (A) Nox4 siRNA reduced the basal Nox4 mRNA and protein expression. (B) Nox4 siRNA remarkably impaired total ROS generation measured by Amplex red assay in the absence and presence $CoCl_2$ (100 μM). (C) Silencing Nox4 expression rescued α-MSH-induced apoptosis plus $CoCl_2$ challenge compared to the control siRNA group. Data are expressed as means ± SEM from triplicate experiments. $^{*}p < 0.05$, $^{**}p < 0.01$, $\#p < 0.01$.

Tissue oxygenation is an important component of the tumor microenvironment and contributes to melanocyte transformation and melanoma development [32]. A hypoxic microenvironment is a widespread phenomenon in tumors, especially in solid tumors [2]. Our data showed that POMC gene delivery rendered melanoma cells more susceptible to hypoxia-induced damage. Several studies have shown that accumulation of ROS was a major regulator to restrain downstream PI3K/AKT signaling pathways and regressed the Bcl-2/Bax ratio in melanoma [33,34]. Excess ROS generation can cause apoptosis by triggering the opening of the mitochondrial permeability transition pore and release of proapoptotic factors [11,12]. Our data revealed that the overload of ROS generation was a main operator for POMC-induced apoptosis in melanoma cells during hypoxia. However, whether other sources of extracellular ROS generation from infiltrating neutrophils or phagocytes are involved in apoptosis in tumor hypoxic regions requires further investigation.

Several sources of ROS including mitochondrial enzymes and NADPH oxidase have been reported in melanoma cells [27]. A previous study found that the expression of the NADPH oxidase components p22phox and Nox4 was required to transform and promote malignant growth in human malignant melanoma cells [31]. Yamaura et al. [35] also demonstrated that Nox4-mediated ROS generation contributed to proliferation and transformation of the melanoma phenotype by regulating G2–M cell cycle progression. In addition, suppression of NADPH oxidase activity by targeting subunits Rac1 and p47phox was found to promote melanogenic differentiation in B16 melanoma cells [36]. We recently demonstrated that the NADPH oxidase isoform Nox4 was a major source of ROS generation upon α-MSH stimulation. Nox4 acts as a feedback mechanism to control melanogenic differentiation by suppressing microphthalmia-associated transcription factor (MITF)-mediated tyrosinase mRNA expression [24]. Here, our data show that the POMC-induced apoptosis under hypoxic conditions was mediated by an upregulation of Nox4. The POMC-derived peptide α-MSH was found to stimulate ROS generation during hypoxia and this contributes to inducing apoptosis in POMC gene therapy in melanoma. Suppressing Nox4 expression by siRNA or scavenging ROS accumulation by NAC reduced apoptosis in POMC gene delivery or α-MSH-treated melanoma cells, pinpointing the role of Nox4-derived ROS in POMC-induced cell apoptosis. However, the precise molecular mechanism of how Nox4-derived ROS induced apoptosis by POMC gene delivery in melanoma cells remained unclear.

The melanocortin 1 receptor (MC1R) is one of the melanocortin receptors that has been shown to have a high binding affinity for its ligand α-MSH, and MC1R is implicated in several physiological functions including pigmentation and inflammation [37]. In all of these regulatory signaling pathways it has been shown that the secondary messenger cAMP-triggered downstream effector molecules protein kinase A (PKA) and cAMP-responsive element binding protein 1 transcription factor promote MITF in melanogenic differentiation [38]. Our recent study also demonstrated that upregulation of Nox4 and ROS generation occurred through the MC1R/PKA/MITF pathway in melanoma cells [24]. In the present study, our data show that POMC gene delivery triggered ROS production, possibly through α-MSH, β-MSH, and ACTH peptides, which have high binding affinity to MC1R. Therefore, POMC-derived peptide α-MSH, β-MSH, and ACTH induction of Nox4-derived ROS is probably driven by the MC1R/cAMP/PKA/MITF pathway. However, the precise molecular mechanisms still need further evaluation.

In summary, we showed that Nox4-mediated ROS generation was a major cause of apoptosis induced by POMC-derived peptides during hypoxic insult. These observations provide a better understanding at the molecular level of the hypoxic conditions in the tumor environment. Our results provide an understanding of tumor-suppressive mechanisms of POMC in mouse B16-F10 melanoma cells, which may facilitate a novel therapy for melanoma control.

Acknowledgments

This work was supported by grants from the National Science Council, Taiwan (NSC 100–2325-B-110-002-MY3), Kaohsiung Veterans General Hospital, Taiwan (MF-DLC 98029S4 and MF-DLC 99053S4), National Sun Yat-Sen University, and the Ophthalmic Research Institute of Australia. G.S.L. receives the Early Career Researcher Fellowship (from University of Melbourne). G.J.D. receives a Principal Research Fellowship from NHMRC. G.S.L. and E.C.C. are supported by The Ansell Ophthalmology Foundation. J.C.W. is supported by the Graduate Program in Marine Biotechnology. The Centre for Eye Research Australia receives operational infrastructure support from the Victorian government.

Appendix A. Supplementary materials

Supplementary data associated with this article can be found in the online version at http://dx.doi.org/10.1016/j.freeradbiomed.2013.12.024.

References

[1] Michaylira, C. Z.; Nakagawa, H. Hypoxic microenvironment as a cradle for melanoma development and progression. *Cancer Biol. Ther.* **5:**476–479; 2006.
[2] Vaupel, P.; Mayer, A. Hypoxia in cancer: significance and impact on clinical outcome. *Cancer Metastasis Rev.* **26:**225–239; 2007.
[3] Lartigau, E.; Randrianarivelo, H.; Avril, M. F.; Margulis, A.; Spatz, A.; Eschwege, F.; Guichard, M. Intratumoral oxygen tension in metastatic melanoma. *Melanoma Res.* **7:**400–406; 1997.
[4] Graeber, T. G.; Osmanian, C.; Jacks, T.; Housman, D. E.; Koch, C. J.; Lowe, S. W.; Giaccia, A. J. Hypoxia-mediated selection of cells with diminished apoptotic potential in solid tumours. *Nature* **379:**88–91; 1996.
[5] Rofstad, E. K.; Danielsen, T. Hypoxia-induced angiogenesis and vascular endothelial growth factor secretion in human melanoma. *Br. J. Cancer* **77:**897–902; 1998.
[6] Finkel, T. Signal transduction by reactive oxygen species. *J. Cell Biol.* **194:**7–15; 2011.
[7] Fruehauf, J. P.; Meyskens Jr. F. L. Reactive oxygen species: a breath of life or death? *Clin. Cancer Res.* **13:**789–794; 2007.
[8] Guzy, R. D.; Schumacker, P. T. Oxygen sensing by mitochondria at complex III: the paradox of increased reactive oxygen species during hypoxia. *Exp. Physiol.* **91:**807–819; 2006.
[9] Chandel, N. S.; Maltepe, E.; Goldwasser, E.; Mathieu, C. E.; Simon, M. C.; Schumacker, P. T. Mitochondrial reactive oxygen species trigger hypoxia-induced transcription. *Proc. Natl. Acad. Sci. USA* **95:**11715–11720; 1998.
[10] Galanis, A.; Pappa, A.; Giannakakis, A.; Lanitis, E.; Dangaj, D.; Sandaltzopoulos, R. Reactive oxygen species and HIF-1 signalling in cancer. *Cancer Lett.* **266:**12–20; 2008.
[11] Fleury, C.; Mignotte, B.; Vayssiere, J. L. Mitochondrial reactive oxygen species in cell death signaling. *Biochimie* **84:**131–141; 2002.
[12] Brenner, C.; Grimm, S. The permeability transition pore complex in cancer cell death. *Oncogene* **25:**4744–4756; 2006.
[13] Raffin-Sanson, M. L.; de Keyzer, Y.; Bertagna, X. Proopiomelanocortin, a polypeptide precursor with multiple functions: from physiology to pathological conditions. *Eur. J. Endocrinol.* **149:**79–90; 2003.
[14] Garfield, A. S.; Lam, D. D.; Marston, O. J.; Przydzial, M. J.; Heisler, L. K. Role of central melanocortin pathways in energy homeostasis. *Trends Endocrinol. Metab.* **20:**203–215; 2009.
[15] Hegadoren, K. M.; O'Donnell, T.; Lanius, R.; Coupland, N. J.; Lacaze-Masmonteil, N. The role of beta-endorphin in the pathophysiology of major depression. *Neuropeptides* **43:**341–353; 2009.
[16] Rousseau, K.; Kauser, S.; Pritchard, L. E.; Warhurst, A.; Oliver, R. L.; Slominski, A.; Wei, E. T.; Thody, A. J.; Tobin, D. J.; White, A. Proopiomelanocortin (POMC), the ACTH/melanocortin precursor, is secreted by human epidermal keratinocytes and melanocytes and stimulates melanogenesis. *FASEB J* **21:**1844–1856; 2007.
[17] Smalley, K.; Eisen, T. The involvement of p38 mitogen-activated protein kinase in the alpha-melanocyte stimulating hormone (alpha-MSH)-induced melanogenic and anti-proliferative effects in B16 murine melanoma cells. *FEBS Lett* **476:**198–202; 2000.
[18] Murata, J.; Ayukawa, K.; Ogasawara, M.; Fujii, H.; Saiki, I. Alpha-melanocyte-stimulating hormone blocks invasion of reconstituted basement membrane (Matrigel) by murine B16 melanoma cells. *Invasion Metastasis* **17:**82–93; 1997.
[19] Liu, G. S.; Tsai, H. E.; Weng, W. T.; Liu, L. F.; Weng, C. H.; Chuang, M. R.; Lam, H. C.; Wu, C. S.; Tee, R.; Wen, Z. H.; Howng, S. L.; Tai, M. H. Systemic pro-opiomelanocortin expression induces melanogenic differentiation and inhibits tumor angiogenesis in established mouse melanoma. *Hum. Gene Ther.* **22:** 325–335; 2011.
[20] Tsai, H. E.; Liu, G. S.; Kung, M. L.; Liu, L. F.; Wu, J. C.; Tang, C. H.; Huang, C. H.; Chen, S. C.; Lam, H. C.; Wu, C. S.; Tai, M. H. Downregulation of hepatoma-derived growth factor contributes to retarded lung metastasis via inhibition of epithelial–mesenchymal transition by systemic POMC gene delivery in melanoma. *Mol. Cancer Ther* **12:**1016–1025; 2013.
[21] Tsai, H. E.; Liu, L. F.; Dusting, G. J.; Weng, W. T.; Chen, S. C.; Kung, M. L.; Tee, R.; Liu, G. S.; Tai, M. H. Pro-opiomelanocortin gene delivery suppresses the growth of established Lewis lung carcinoma through a melanocortin-1 receptor-independent pathway. *J. Gene Med.* **14:**44–53; 2012.
[22] Liu, G. S.; Liu, L. F.; Lin, C. J.; Tseng, J. C.; Chuang, M. J.; Lam, H. C.; Lee, J. K.; Yang, L. C.; Chan, J. H.; Howng, S. L.; Tai, M. H. Gene transfer of pro-opiomelanocortin prohormone suppressed the growth and metastasis of melanoma: involvement of alpha-melanocyte-stimulating hormone-mediated inhibition of the nuclear factor kappaB/cyclooxygenase-2 pathway. *Mol. Pharmacol.* **69:**440–451; 2006.
[23] Hsiao, S. T.; Lokmic, Z.; Peshavariya, H.; Abberton, K. M.; Dusting, G. J.; Lim, S. Y.; Dilley, R. J. Hypoxic conditioning enhances the angiogenic paracrine activity of human adipose-derived stem cells. *Stem Cells Dev.* **22:**1614–1623; 2013.
[24] Liu, G. S.; Peshavariya, H.; Higuchi, M.; Brewer, A. C.; Chang, C. W.; Chan, E. C.; Dusting, G. J. Microphthalmia-associated transcription factor modulates expression of NADPH oxidase type 4: a negative regulator of melanogenesis. *Free Radic. Biol. Med.* **52:**1835–1843; 2012.
[25] Zhang, P.; Li, W.; Li, L.; Wang, N.; Li, X.; Gao, M.; Zheng, J.; Lei, S.; Chen, X.; Lu, H.; Liu, Y. Treatment with edaravone attenuates ischemic brain injury and inhibits neurogenesis in the subventricular zone of adult rats after focal cerebral ischemia and reperfusion injury. *Neuroscience* **201:**297–306; 2012.
[26] Tochigi, M.; Inoue, T.; Suzuki-Karasaki, M.; Ochiai, T.; Ra, C.; Suzuki-Karasaki, Y. Hydrogen peroxide induces cell death in human TRAIL-resistant melanoma through intracellular superoxide generation. *Int. J. Oncol.* **42:**863–872; 2013.
[27] Wittgen, H. G.; van Kempen, L. C. Reactive oxygen species in melanoma and its therapeutic implications. *Melanoma Res.* **17:**400–409; 2007.
[28] Valverde, P.; Manning, P.; McNeil, C. J.; Thody, A. J. Activation of tyrosinase reduces the cytotoxic effects of the superoxide anion in B16 mouse melanoma cells. *Pigm. Cell Res.* **9:**77–84; 1996.
[29] Barbi de Moura, M.; Vincent, G.; Fayewicz, S. L.; Bateman, N. W.; Hood, B. L.; Sun, M.; Suhan, J.; Duensing, S.; Yin, Y.; Sander, C.; Kirkwood, J. M.; Becker, D.; Conrads, T. P.; Van Houten, B.; Moschos, S. J. Mitochondrial respiration—an important therapeutic target in melanoma. *PLoS One* **7:**e40690; 2012.
[30] Denkert, C.; Kobel, M.; Berger, S.; Siegert, A.; Leclere, A.; Trefzer, U.; Hauptmann, S. Expression of cyclooxygenase 2 in human malignant melanoma. *Cancer Res.* **61:**303–308; 2001.
[31] Brar, S. S.; Kennedy, T. P.; Sturrock, A. B.; Huecksteadt, T. P.; Quinn, M. T.; Whorton, A. R.; Hoidal, J. R. An NAD(P)H oxidase regulates growth and transcription in melanoma cells. *Am. J. Physiol. Cell Physiol* **282:**C1212–1224; 2002.
[32] Bedogni, B.; Powell, M. B. Hypoxia, melanocytes and melanoma—survival and tumor development in the permissive microenvironment of the skin. *Pigm. Cell Melanoma Res* **22:**166–174; 2009.
[33] Lee, J. H.; Won, Y. S.; Park, K. H.; Lee, M. K.; Tachibana, H.; Yamada, K.; Seo, K. I. Celastrol inhibits growth and induces apoptotic cell death in melanoma cells via the activation ROS-dependent mitochondrial pathway and the suppression of PI3K/AKT signaling. *Apoptosis* **17:**1275–1286; 2012.
[34] Mayola, E.; Gallerne, C.; Esposti, D. D.; Martel, C.; Pervaiz, S.; Larue, L.; Debuire, B.; Lemoine, A.; Brenner, C.; Lemaire, C. Withaferin A induces apoptosis in human melanoma cells through generation of reactive oxygen species and down-regulation of Bcl-2. *Apoptosis* **16:**1014–1027; 2011.
[35] Yamaura, M.; Mitsushita, J.; Furuta, S.; Kiniwa, Y.; Ashida, A.; Goto, Y.; Shang, W. H.; Kubodera, M.; Kato, M.; Takata, M.; Saida, T.; Kamata, T. NADPH oxidase 4 contributes to transformation phenotype of melanoma cells by regulating G2–M cell cycle progression. *Cancer Res.* **69:**2647–2654; 2009.
[36] Zhao, Y.; Liu, J.; McMartin, K. E. Inhibition of NADPH oxidase activity promotes differentiation of B16 melanoma cells. *Oncol. Rep.* **19:**1225–1230; 2008.
[37] Lasaga, M.; Debeljuk, L.; Durand, D.; Scimonelli, T. N.; Caruso, C. Role of alpha-melanocyte stimulating hormone and melanocortin 4 receptor in brain inflammation. *Peptides* **29:**1825–1835; 2008.
[38] Bertolotto, C.; Abbe, P.; Hemesath, T. J.; Bille, K.; Fisher, D. E.; Ortonne, J. P.; Ballotti, R. Microphthalmia gene product as a signal transducer in cAMP-induced differentiation of melanocytes. *J. Cell Biol.* **142:**827–835; 1998.